

Supplementary Information

Erythrocyte membrane-modified biomimetic synergistic nanosystem for cancer anti-vascular therapy and initial efficacy monitoring

Jieying Zhang,^a Fang Li,^a Lili Su,^b Qian Hu,^a Jianfeng Li^{*b} and Xingjun Zhu^{*a}

^a School of Physical Science and Technology, ShanghaiTech University, 393 Huaxia Road, Shanghai, 201210, P. R. China.

E-mail: zhuxj1@shanghaitech.edu.cn

^b Gene Editing Center, School of Life Science and Technology, ShanghaiTech University, 393 Huaxia Road, Shanghai, 201210, P. R. China.

E-mail: lijf1@shanghaitech.edu.cn

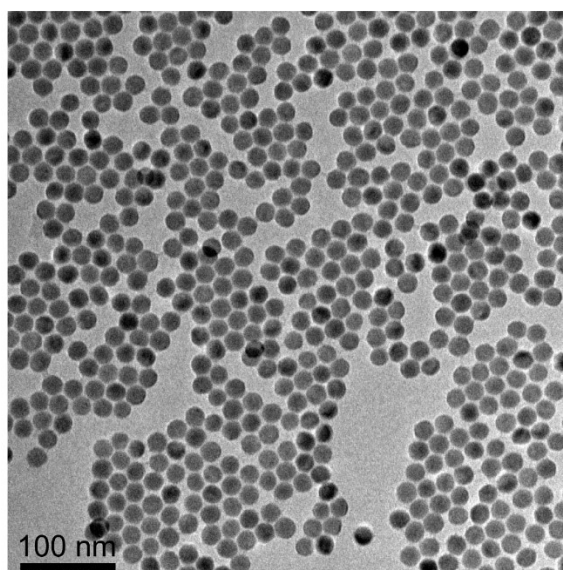


Figure S1. Transmission electron microscope (TEM) images of NaYF₄:Yb,Er nanoparticles.

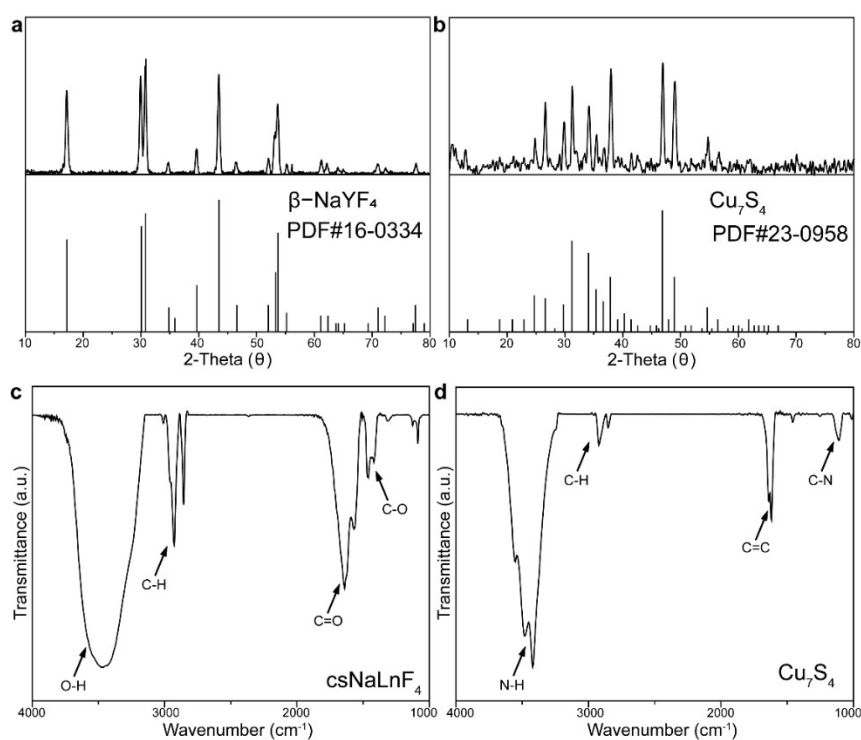


Figure S2. X-ray powder diffraction (XRD) patterns of (a) NaYF₄:20%Yb,2%Er@NaLuF₄ (csNaLnF₄) and (b) Cu₇S₄ nanoparticles. Fourier transformed infrared (FTIR) spectra of (c) csNaLnF₄ and (d) Cu₇S₄ nanoparticles.

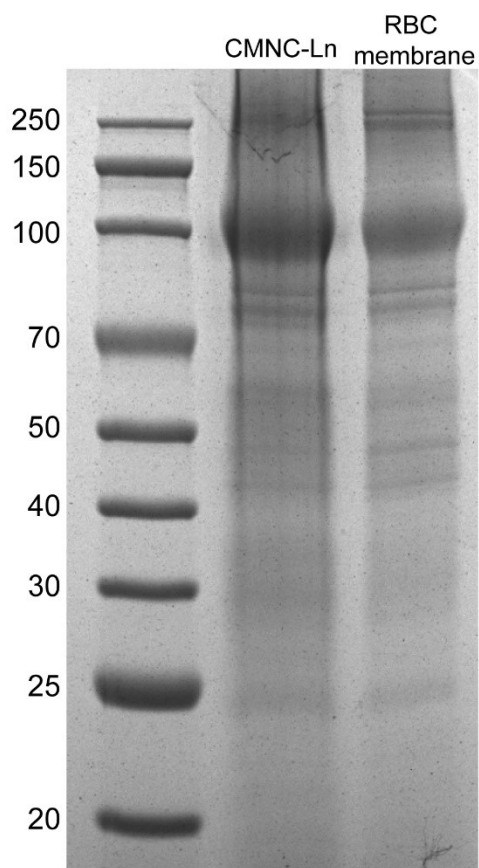


Figure S3. SDS-PAGE protein analysis of CMNC-Ln and RBC membrane.

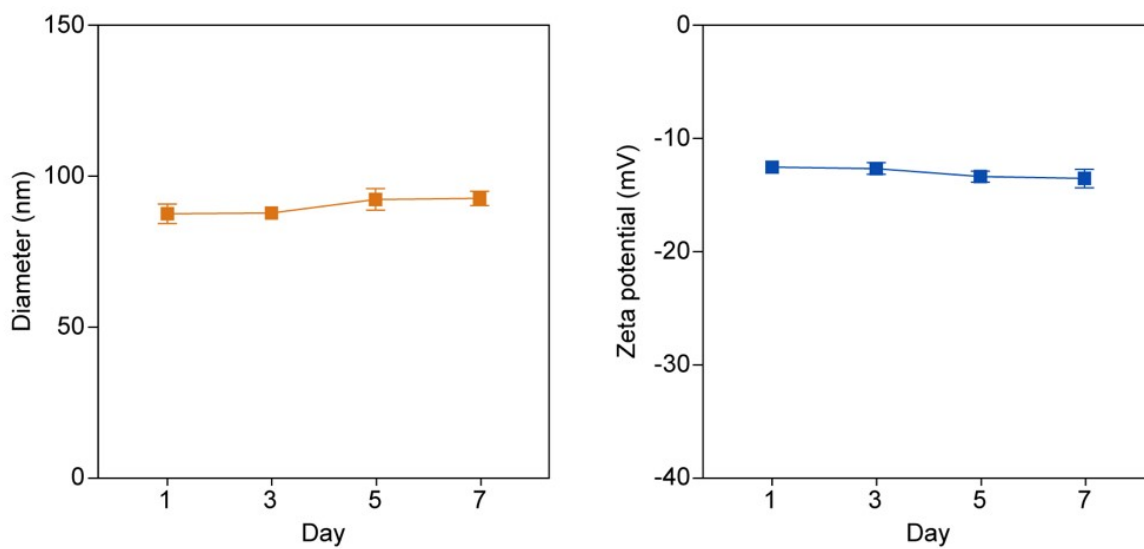


Figure S4. Dynamic light scattering (DLS) and Zeta potential analysis of CMNC-Ln in one week after synthesis. Error bar stands for s. d. from $n = 3$ replicated samples.

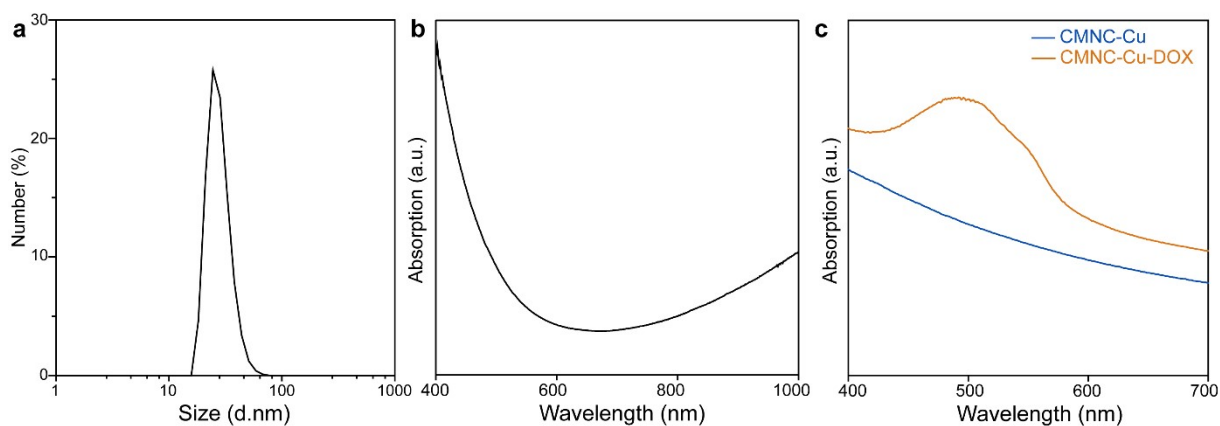


Figure S5. (a) Size distribution of Cu₇S₄ nanoparticles in tetrahydrofuran. (b) Absorption spectrum of Cu₇S₄ nanoparticles. (c) The comparison of the absorption spectra of RBC membrane coated nanocomposite with Cu₇S₄ nanoparticles (CMNC-Cu) (before) and after doxorubicin loading (CMNC-Cu-DOX).

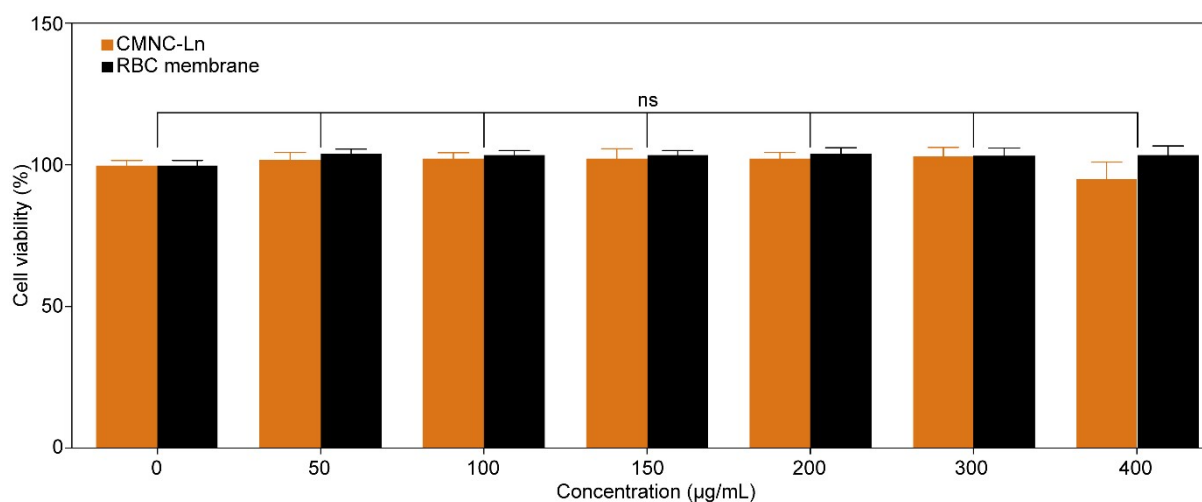


Figure S6. Characterizations of cytotoxicity of CMNC-Ln. Cell viability was measured via MTT assay of HEK 293T cells treated with a single nanoparticle and multiple nanoparticles loaded CMNC-Ln at different concentrations (0, 50, 100, 150, 200, 300, 400 µg ml⁻¹). Cells treated with pure erythrocyte membrane at different concentrations (0, 50, 100, 150, 200, 300, 400 µg ml⁻¹) was set as control. No significant difference was observed in all groups.

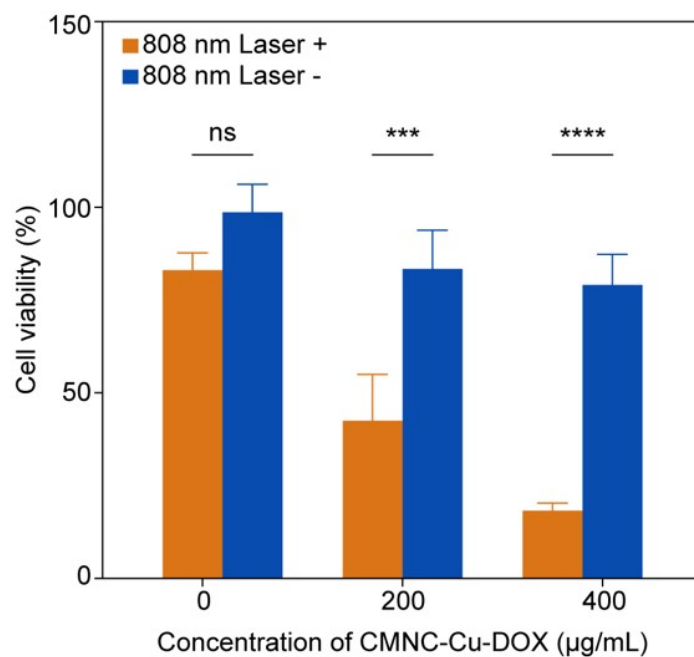


Figure S7. Demonstration of *in vitro* anti-tumor treatment efficacy. Cell viability was measured via MTT assay of 4T1 cells treated with CMNC-Cu-DOX at different concentrations (0, 200, 400 µg ml⁻¹) and irradiated by a continuous wave 808 nm laser. Cells treated with CMNC-Cu-DOX at different concentrations (0, 200, 400 µg ml⁻¹) without irradiation of the laser are set as control.

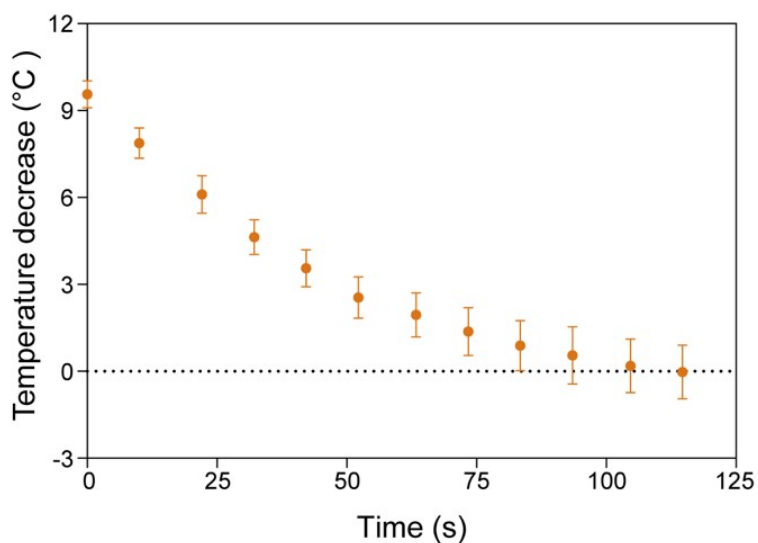


Figure S8. Temperature decrease of the mice tumor with CMNC-Cu-DOX injection and irradiation of a 808 nm laser for 30 min. Error bar stands for s. d. from n = 3 replicated samples.

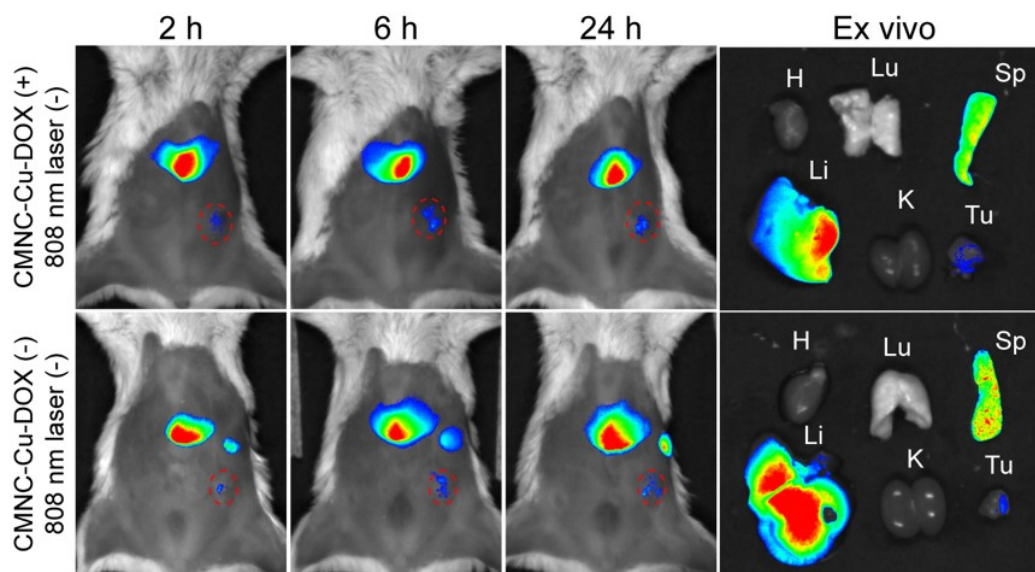


Figure S9. Whole body NIR-II imaging of tumor-bearing mouse and the main organs (heart (H), lung (Lu), liver (Li), spleen (Sp), kidney (K) and tumor (Tu)) with only CMNC-Cu-DOX injection or without any treatment. The tumor-bearing mice were injected with CMNC-Ln and the NIR-II luminescence was excited by a 980 nm laser with a 1300 nm long-pass filter. Tumors were marked with red circle.

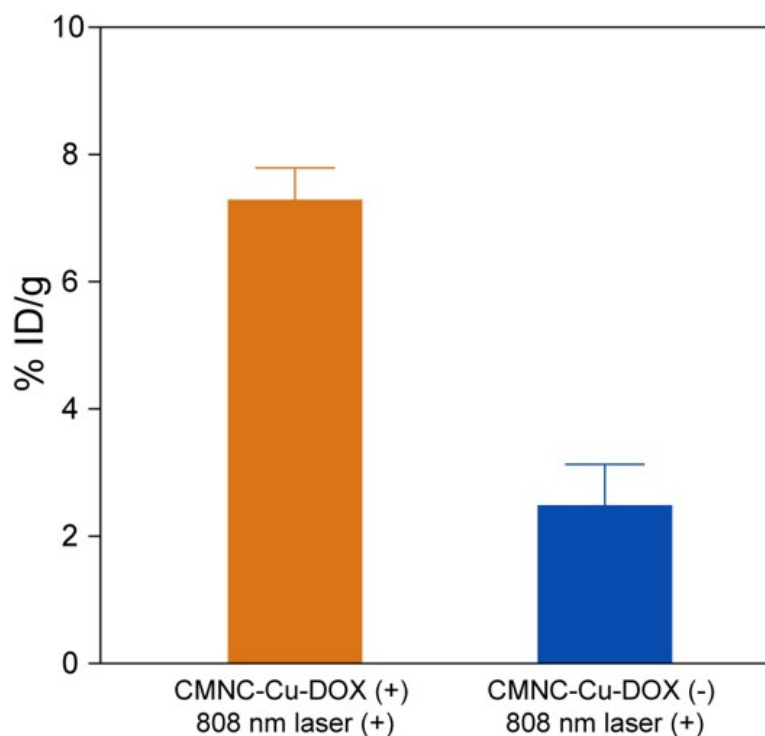


Figure S10. Accumulation of CMNC-Ln in the tumors of mice with or without anti-vascular treatment determined by inductively coupled plasma atomic emission spectroscopy (ICP-AES). The quantities of CMNC-Ln in the tumors are shown in percentage injected dose per gram of tissue (%ID/g).

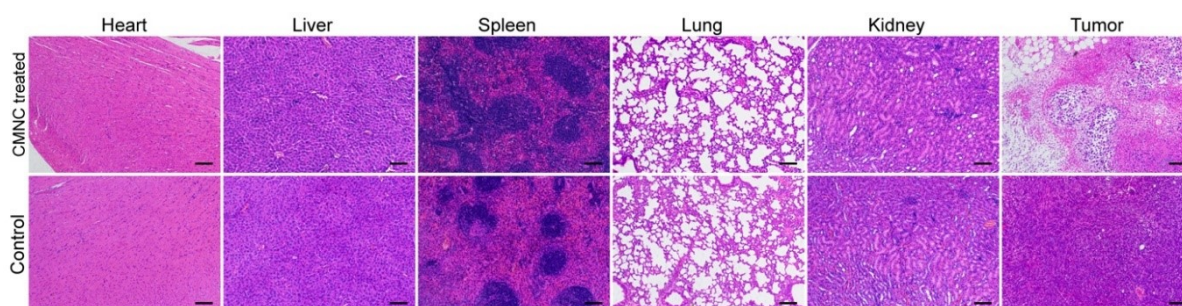


Figure S11. Histological analysis in the heart, liver, spleen, lung, kidney and tumor of tumor-bearing mice injected with CMNC-Cu-DOX under an 808 nm laser irradiation. The organs were stained with hematoxylin and eosin (H&E), and scale bars were defined as 100 μ m.

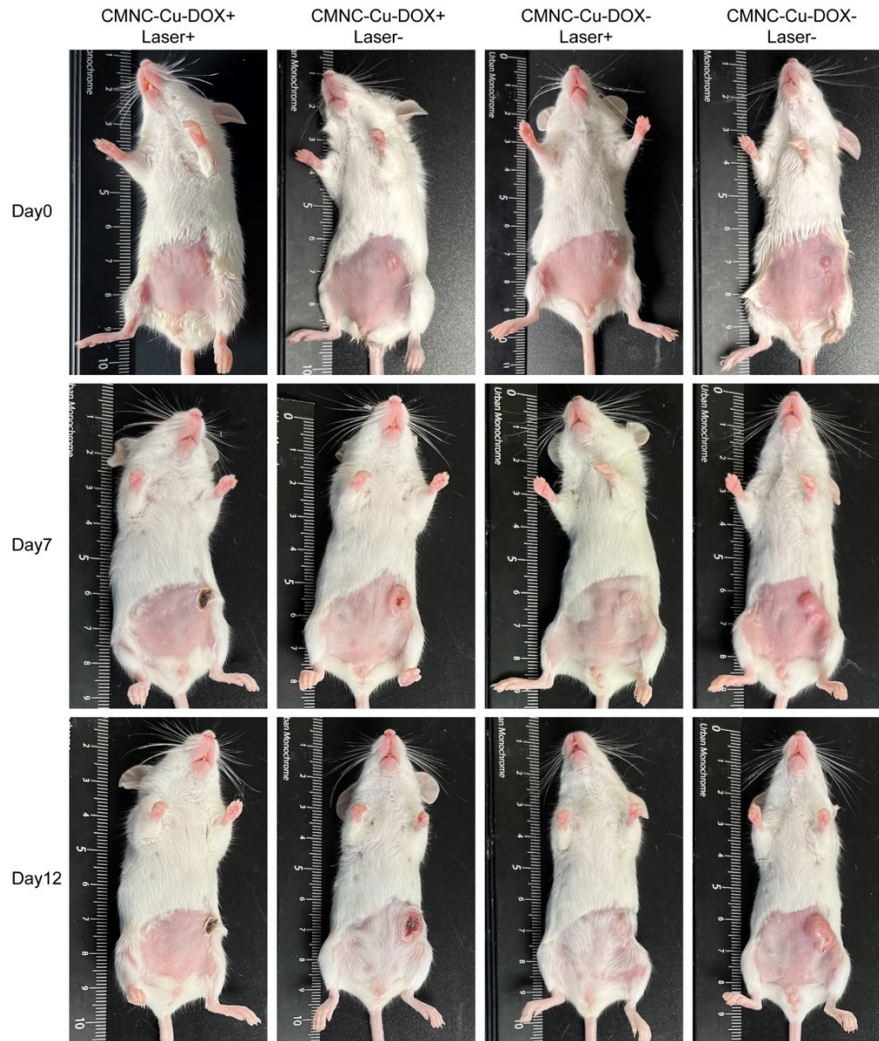


Figure S12. Anti-vascular therapy in vivo. Representative photos of tumor-bearing mice in different treatment phases.